# Supplementary Information

## The Synergy between Metal Facet and Oxide Support Facet for Enhanced Catalytic Performance: The Case of Pd-$TiO_2$

Muhan Cao, [†] Zeyuan Tang, [†] Qipeng Liu, [†] Yong Xu, [†] Min Chen, [†] Haiping Lin,*, [†] Youyong Li, [†] Elad Gross,[‡] Qiao Zhang*,[†]

[†] Institute of Functional Nano & Soft Materials (FUNSOM), Jiangsu Key Laboratory for Carbon-Based Functional Materials & Devices, Soochow University, 199 Ren'ai Road, Suzhou, 215123, Jiangsu, PR China

[‡] Institute of Chemistry, the Hebrew University of Jerusalem, Jerusalem 9190401, Israel

E-mail: hplin@suda.edu.cn (H.L.); qiaozhang@suda.edu.cn (Q.Z.)

M.C., Z.T. and Q.L. contributed equally to this paper.

### Experimental Section

**Synthesis of Pd nanocubes and octahedrons.** The synthesis of Pd nanocubes and octahedrons has been achieved through one-pot method.[1-3] In the presence of surfactant and shape-directing agents (KBr for nanocubes[1] and citric acid for octahedrons[2, 3]), Pd nanocubes and octahedrons with a uniform size distribution can be obtained. In a typical synthesis procedure of Pd nanocubes, 105 mg of PVP (M.W.=55,000, Sigma-Aldrich, 856568-100g), 60 mg of L-ascorbic acid (Sigma-Aldrich, 33034-100g) and 300 mg of KBr (Sigma-Aldrich, 60093-250g) were added into 8 mL of water in a 20 mL vial, and pre-heated in air under stirring at 80 °C. Then, 3 mL of an aqueous solution containing 57 mg of $Na_2PdCl_4$ (Sigma-Aldrich, 205818-5g) was quickly injected into the vial through a pipette. The vial was then capped, and heated at 80 °C for 3 h. The resulting product was collected by centrifugation and washed by acetone and ethanol for several times. For the Pd octahedrons with a size of ~26 nm, they were synthesized as follows: 256 mg of cetanecyl trimethyl ammonium chloride (CTAC, TCI, H0082) was dissolved in 8 mL of water in a 3-neck flask, 60 mg of L-ascorbic acid and 60 mg of citric acid (Aladdin,

C108873-500g) were added into the flask and pre-heated at 100 °C. An aqueous solution of 60 mg of $Na_2PdCl_4$ in 3 mL of water was injected into the flask through a pipette. The mixture solution was allowed to proceed at 100 °C for another 3 h. The obtained product was washed by water for several time, and finally dispersed in water. For the Pd octahedrons with a size of ~13 nm, they were synthesized as follows: 105 mg of PVP (M.W.=55,000) was dissolved in 8 mL of water, and then placed in a 3-neck flask which equipped with a reflux condenser. Subsequently, 60 mg of citric acid were added into the flask and pre-heated at 90 °C under vigorous stirring. An aqueous solution of 57 mg of $Na_2PdCl_4$ in 3 mL of water was quickly injected into the flask through a pipette. The mixture solution was allowed to proceed at 90 °C for another 26 h. The obtained product was washed by acetone and ethanol for several times, and finally dispersed in water.

**Synthesis of $TiO_2$ nanosheets with different percentages of exposed (001) facets.** $TiO_2$ nanosheets were prepared by a simple hydrothermal method.[4, 5] 5 mL of titanium butoxide (TBOT, Fluka, 86910-250mL) and a define amount of HF solution (40 wt%) were mixed under stirring and transferred into a Telfon-line 50 mL autoclave, and then kept at 200 °C for 24 h. The product was washed with water for several times and then dried at 60 °C. The percentage of exposed (001) facets was decided by the different amount of HF solution (0.15, 0.3 and 0.4 mL) in the reaction. $TiO_2$ with 2% exposed (001) facet was synthesized through Liu's report.[6]

**Synthesis of Pd-$TiO_2$ hybrid nanocrystals.** The Pd-$TiO_2$ hybridized nanocrystals were obtained through a one-pot procedure similar to the synthesis of Pd nanocubes and octahedrons in the presence of $TiO_2$. P25 (Acros) and $TiO_2$ nanosheets with different percentages of exposed (001) facets were added into the initial 8 mL of water. The other protocols were the same as the above methods. The concentration of Pd was measured by an inductivity-coupled plasma optical emission spectrometry (ICP-OES, Variance, VISTA-MPX).

**ESR analysis.** Aqueous suspension of samples was mixed with 0.5 mL of 2,2,6,6-tetramethyl-4-piperidone hydrochloride (4-oxo-TMP, TCI, T1147-25 g) solution (50 mM). The concentrations of Pd and Pd-$TiO_2$ crystals were selected to

maintain the surface Pd atoms equivalent. The mixed solution was characterized by an ESR (Bruker, EMX-8/2.7) spectroscopy at room temperature.

**Glucose oxidation.** Typically, glucose solution (15 mM) was heated to 50 °C with $O_2$ injection for 15 min to reach oxygen-saturation. Pd nanocrystals were added into the solution, at the same time, a 300 W xenon lamp (Aulight, CEL-HXF300) was employed as the light resource. As a reference, the reactions were also conducted in the dark. The concentrations of Pd and Pd-$TiO_2$ crystals were selected to maintain the surface Pd atoms equivalent. After a certain period, the mixture liquid was filtrated to remove the catalysts. The concentrations of the gluconic acid produced were measured by HPLC (Agilent 1200 Infinity Series) at 200 nm.

**Calculation details**:

The slab setup for Pd-$TiO_2$ systems are listed in Table S1. The hybrid systems are modelled by adsorbing Pd nanorods on $TiO_2$ surfaces in order to minimize lattice mismatch between Pd and $TiO_2$.[7] Based on our calculations, the most optimized anatase $TiO_2$ parameters are: a = b =3.862 Å, c = 9.511 Å. They are in good agreement with other theoretical values[8]: a = b =3.786 Å, c = 9.737 Å. The calculated lattice constant of Pd is: a = 3.977 Å, which is also consisted with the previous calculation[9]: a = 4.014 Å. For $O_2$ adsorption calculations, we adopt the adsorption sites reported by Long and co-workers,[10] namely hollow site for Pd(100) and short-bridge site for Pd(111).

**Table S1**. Structural information of the Pd- $TiO_2$ hybrid systems in DFT calculations

| System | Pd(100) | Pd(111) | $TiO_2$(001) | $TiO_2$(101) | Number of atoms | | |
|---|---|---|---|---|---|---|---|
| | | | | | O | $Pd^-$ | Ti |
| Pd(100)-$TiO_2$(001) | 3x4 | - | 4x3 | - | 96 | 48 | 48 |
| Pd(100)-$TiO_2$(101) | 3x4 | - | - | 2x3 | 192 | 48 | 96 |
| Pd(111)-$TiO_2$(001) | - | 2x8 | 3x5 | - | 120 | 64 | 60 |
| Pd(111)-$TiO_2$(101) | - | 2x8 | - | 1x5 | 160 | 64 | 80 |
| Pd(100) | 3x4 | - | - | - | 0 | 80 | 0 |
| Pd(111) | - | 2x8 | - | - | 0 | 80 | 0 |

For pure Pd surfaces

- Pd: 5 layers

For Pd- $TiO_2$ hybrid systems

- Pd: 4 layers
- $TiO_2$: 4 O-Ti-O layers

**Table S2**. O-O length for different systems

| System | O-O lengths (Å) | | |
|---|---|---|---|
| | $0e^-$ | $1e^-$ | $2e^-$ |
| Pd(100)-$TiO_2$(001) | 1.433 | 1.441 | 1.452 |
| Pd(100)-$TiO_2$(101) | 1.426 | 1.433 | 1.445 |
| Pd(111)-$TiO_2$(001) | 1.371 | 1.382 | 1.430 |
| Pd(111)-$TiO_2$(101) | 1.364 | 1.375 | 1.392 |
| Pd(100) | 1.408 | - | - |
| Pd(111) | 1.340 | - | - |

Table S2 shows the bond length of the adsorbed $O_2$ molecule over the Pd surfaces and Pd-$TiO_2$ hybrid systems. In general, the O-O distances are increased when extra electrons are added. The effect of substrate facets are clearly illustrated: the catalytic activities of Pd-$TiO_2$ is Pd(100)-$TiO_2$(001)> Pd(100)-$TiO_2$(101) > Pd(111)-$TiO_2$(001) > Pd(111)-$TiO_2$(101). Without irradiation, the O-O bond length are not significantly change on the Pd(100) and Pd(100)-$TiO_2$ surfaces. This can be ascribed to the higher surface energy of the Pd(100) surface, in which the electrons are already accumulated at the surface atoms. By contrast, because the Pd(111) surface has a lower surface energy, the effect of charge transfer from the oxide support to the surface Pd atoms is therefore more distinguished.

**Table S3**. Structural information of the as-obtained Pd nanoparticles and $TiO_2$ nanosheets.

| Sample | Average edge (nm) | Percentage of surface atoms | Average thickness (nm) | Percentage of (001) facets |
|---|---|---|---|---|
| Pd nanocubes | 11 | 10.90% | --- | --- |
| Pd octahedrons | 26 | 6.18% | -- | --- |
| $TiO_2$-1 | 18 | --- | 35 | 2% |
| $TiO_2$-2 | 25 | --- | 13 | 39% |
| $TiO_2$-3 | 40 | --- | 10 | 61% |
| $TiO_2$-4 | 68 | --- | 8 | 80% |

[a] The percentage of surface atoms in Pd crystals was calculated according to Long's report.[10] [b] The percentage of exposed (001) facets in $TiO_2$ was calculated as described in previous study.[11]

**Table S4**. Oxidation of glucose by different catalysts with molecular oxygen.

| catalyst | time (min) | yield (%) | $TON_{surf}$ | $TOF_{surf}$ |
|---|---|---|---|---|
| Pd Cubes[#] | 120 | 19.9 | 249 | 2.1 |
| Pd Cubes | 60 | 23.0 | 288 | 4.8 |
| Pd Cubes | 120 | 38.3 | 479 | 4.0 |
| Pd Cubes-P25[#] | 120 | 34.8 | 435 | 3.6 |
| Pd Cubes-P25 | 60 | 40.0 | 500 | 8.3 |
| Pd Cubes-P25 | 120 | 75.4 | 942 | 7.8 |
| Pd Cubes-$TiO_2$-1[#] | 120 | 34.6 | 432 | 3.6 |
| Pd Cubes-$TiO_2$-1 | 60 | 34.0 | 425 | 7.1 |
| Pd Cubes-$TiO_2$-1 | 120 | 51.4 | 642 | 5.4 |
| Pd Cubes-$TiO_2$-2[#] | 120 | 34.6 | 432 | 3.6 |
| Pd Cubes-$TiO_2$-2 | 60 | 67.3 | 841 | 14.0 |
| Pd Cubes-$TiO_2$-2 | 120 | 94.9 | 1186 | 9.9 |
| Pd Cubes-$TiO_2$-3[#] | 120 | 50.4 | 630 | 5 |
| Pd Cubes-$TiO_2$-3 | 60 | 83.1 | 1039 | 17 |
| Pd Cubes-$TiO_2$-3 | 120 | 100 | 1250 | 10 |
| Pd Cubes-$TiO_2$-4[#] | 120 | 51.9 | 649 | 5.4 |
| Pd Cubes-$TiO_2$-4 | 60 | 93.7 | 1171 | 19.5 |
| Pd Cubes-$TiO_2$-4 | 120 | 100 | 1250 | 10.4 |
| Pd octahedrons[#] | 120 | 13.3 | 166 | 1.4 |
| Pd octahedrons | 60 | 6.8 | 85 | 1.4 |
| Pd octahedrons | 120 | 12.9 | 161 | 1.3 |
| Pd Oct-P25[#] | 120 | 22.0 | 275 | 2.3 |
| Pd Oct-P25 | 60 | 23.3 | 291 | 4.8 |
| Pd Oct-P25 | 120 | 29.5 | 369 | 3.1 |
| Pd Oct-$TiO_2$-1[#] | 120 | 19.5 | 244 | 2.0 |
| Pd Oct-$TiO_2$-1 | 60 | 15.4 | 192 | 3.2 |
| Pd Oct-$TiO_2$-1 | 120 | 22.5 | 281 | 2.3 |
| Pd Oct-$TiO_2$-2[#] | 120 | 30.6 | 382 | 3.2 |
| Pd Oct-$TiO_2$-2 | 60 | 29.7 | 371 | 6.2 |
| Pd Oct-$TiO_2$-2 | 120 | 38.4 | 480 | 4 |
| Pd Oct-$TiO_2$-3[#] | 120 | 31.2 | 390 | 3.2 |
| Pd Oct-$TiO_2$-3 | 60 | 32.0 | 400 | 6.7 |
| Pd Oct-$TiO_2$-3 | 120 | 49.1 | 614 | 5.1 |
| Pd Oct-$TiO_2$-4[#] | 120 | 27.6 | 345 | 2.9 |

| | | | | |
|---|---|---|---|---|
| Pd Oct-$TiO_2$-4 | 60 | 29.0 | 362 | 6.0 |
| Pd Oct-$TiO_2$-4 | 120 | 55.8 | 698 | 5.8 |
| P25 | 120 | 2.8 | 35 | 0.3 |
| $TiO_2$-1 | 120 | 4.4 | 55 | 0.4 |
| $TiO_2$-2 | 120 | 2.2 | 28 | 0.2 |
| $TiO_2$-3 | 120 | 4.9 | 61 | 0.5 |
| $TiO_2$-4 | 120 | 3.1 | 39 | 0.3 |
| Pd Cubes* | 60 | 11.4 | 142 | 2.4 |
| Pd Cubes* | 120 | 11.8 | 148 | 1.2 |
| Pd Cubes-P25* | 60 | 8.6 | 108 | 1.8 |
| Pd Cubes-P25* | 120 | 12.0 | 150 | 1.2 |
| Pd Cubes-$TiO_2$-1* | 60 | 10.8 | 135 | 2.2 |
| Pd Cubes-$TiO_2$-1* | 120 | 16.7 | 209 | 1.7 |
| Pd Cubes-$TiO_2$-2* | 60 | 15.3 | 191 | 3.2 |
| Pd Cubes-$TiO_2$-2* | 120 | 15.2 | 190 | 1.6 |
| Pd Cubes-$TiO_2$-3* | 60 | 11.1 | 139 | 2.3 |
| Pd Cubes-$TiO_2$-3* | 120 | 15.4 | 192 | 1.6 |
| Pd Cubes-$TiO_2$-4* | 60 | 14.0 | 175 | 2.9 |
| Pd Cubes-$TiO_2$-4* | 120 | 16.9 | 211 | 1.8 |
| Pd octahedrons* | 60 | 5.1 | 64 | 1.1 |
| Pd octahedrons* | 120 | 4.8 | 60 | 0.5 |
| Pd Oct-P25* | 60 | 3.0 | 38 | 0.6 |
| Pd Oct-P25* | 120 | 4.4 | 55 | 0.4 |
| Pd Oct-$TiO_2$-1* | 60 | 6.7 | 84 | 1.4 |
| Pd Oct-$TiO_2$-1* | 120 | 6.4 | 80 | 0.7 |
| Pd Oct-$TiO_2$-2* | 60 | 5.0 | 62 | 1.0 |
| Pd Oct-$TiO_2$-2* | 120 | 5.4 | 68 | 0.6 |
| Pd Oct-$TiO_2$-3* | 60 | 8.9 | 111 | 1.8 |
| Pd Oct-$TiO_2$-3* | 120 | 6.3 | 79 | 0.6 |
| Pd Oct-$TiO_2$-4* | 60 | 7.7 | 96 | 1.6 |
| Pd Oct-$TiO_2$-4* | 120 | 9.0 | 112 | 0.9 |

[#]The catalytic reactions were carried out in dark. *Addition of excess amount of carotene as singlet $O_2$ scavenger. Reaction conditions: $mol_{surface}$: 0.8‰ for both Pd nanocubes and octahedrons.

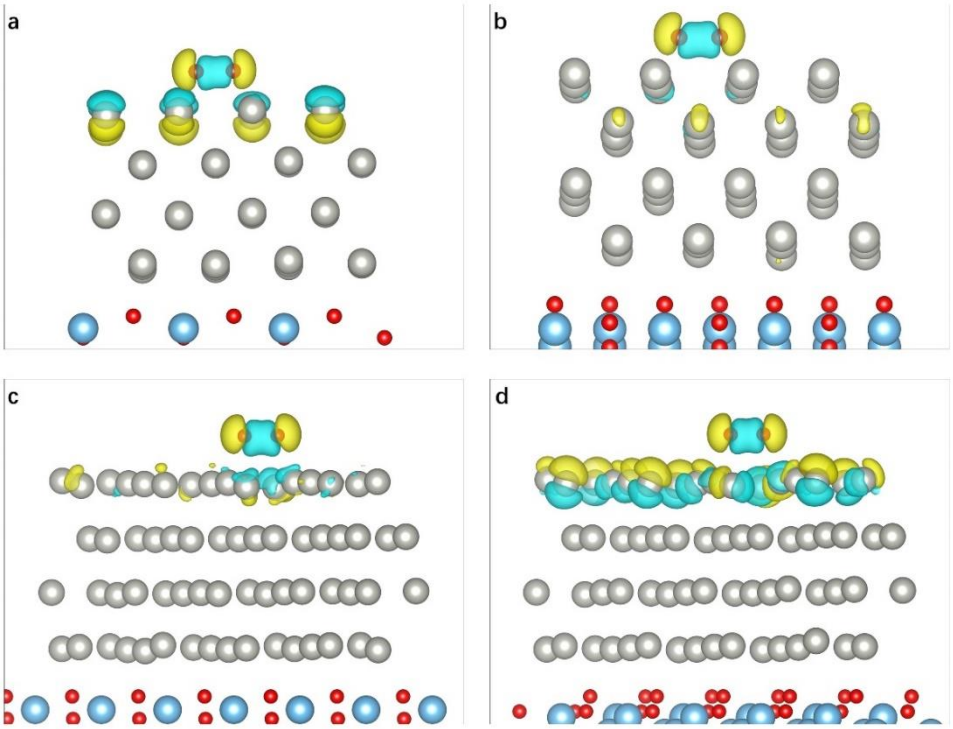


**Figure S1**. Charge density differences of Pd-$TiO_2$ systems: (a) Pd(100)-$TiO_2$(001), (b) Pd(100)-$TiO_2$(101), (c) Pd(111)-$TiO_2$(001), (d) Pd(111)-$TiO_2$(101). $\Delta\rho$ = $\rho$(charged system)-$\rho$(neutral system). The contour values are ±0.001e/a.u.$^3$, yellow: charge aggregation, blue: charge dispersion.

Figure S1 shows the electronic density redistribution, $\Delta\rho$, under irradiation. As seen, when hot electrons are created, they are transferred to the anti-bonding orbital of the adsorbed $O_2$ molecules.

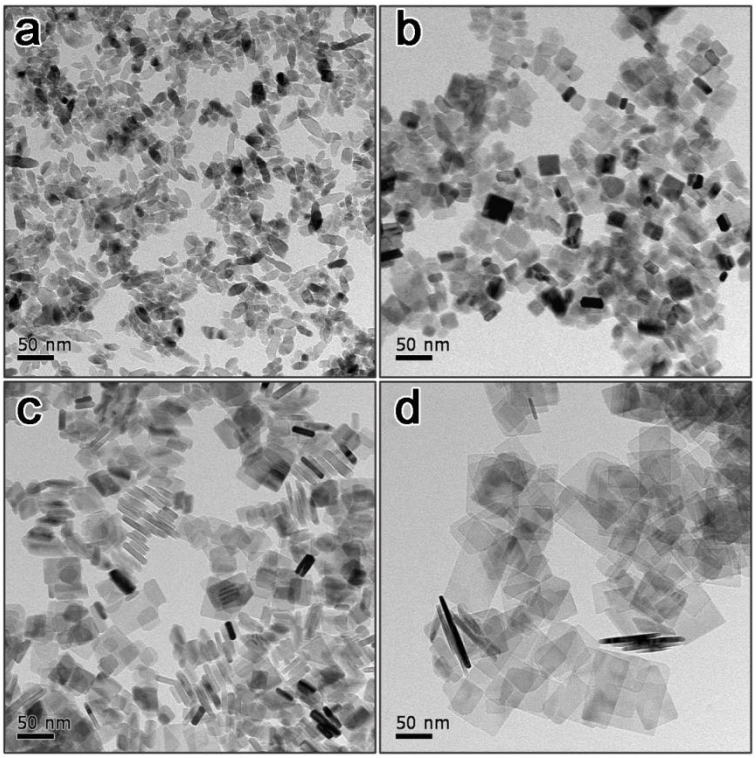


**Figure S2**. TEM images of (a) $TiO_2$-1, (b) $TiO_2$-2, (c) $TiO_2$-3 and (d) $TiO_2$-4.

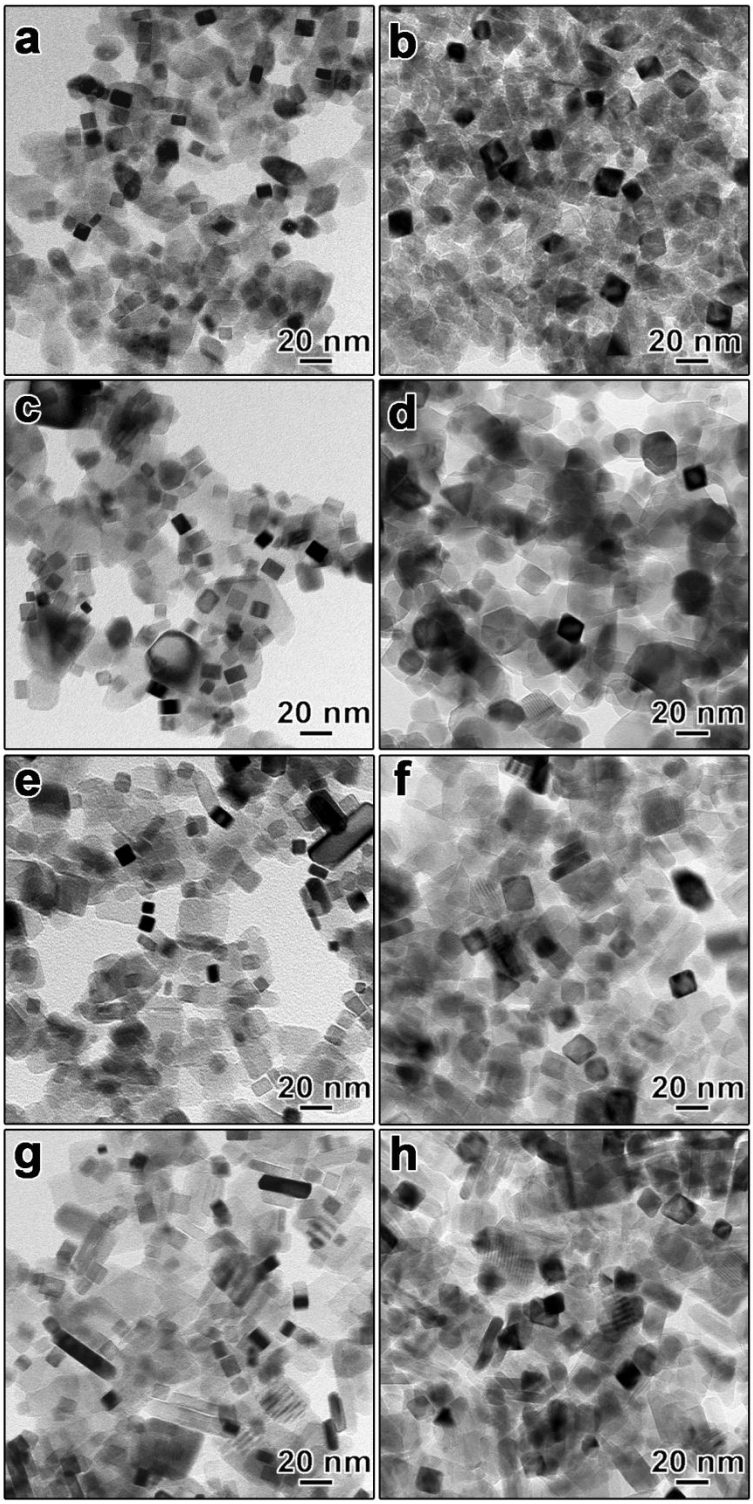


**Figure S3**. TEM images of (a) Pd Cubes-$TiO_2$-1, (b) Pd Oct-$TiO_2$-1, (c) Pd Cubes-P25, (d) Pd Oct-P25, (e) Pd Cubes-$TiO_2$-2, (f) Pd Oct-$TiO_2$-2, (g) Pd Cubes-$TiO_2$-3 and (h) Pd Oct-$TiO_2$-3.

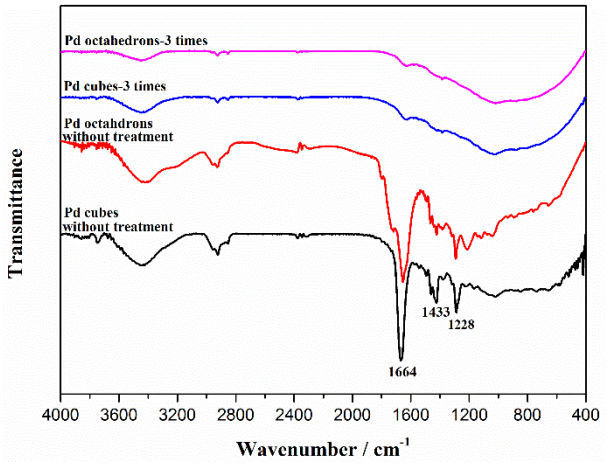


**Figure S4.** FTIR spectra of Pd cubes and octahedrons without any treatments and after washing by acetone and ethanol for three times.

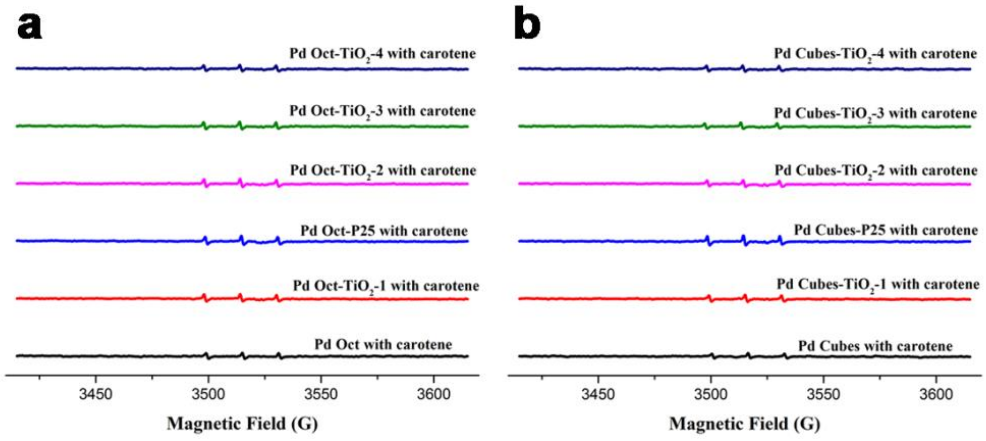


**Figure S5.** ESR spectra of (a) Pd nanocubes- and (b) Pd octahedron-based samples in the presence of 4-oxo-TMP using carotene as the scavenger for singlet $O_2$.

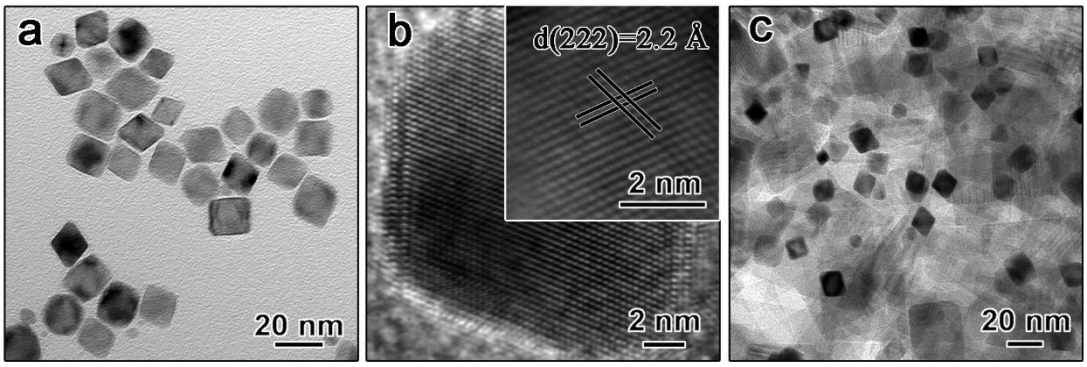


**Figure S6**. TEM images showing (a, b) Pd octahedrons with size around 13 nm and (c) the composite of Pd octahedrons with $TiO_2$ nanosheets.

## References

1. Jin, M.; Liu, H.; Zhang, H.; Xie, Z.; Liu, J.; Xia, Y. *Nano Res.* **2010,** 4, 83-91.
2. Kim, M.; Kim, Y.; Hong, J. W.; Ahn, S.; Kim, W. Y.; Han, S. W. *Chem. Commun.* **2014,** 50, 9454-9457.
3. Lim, B.; Xiong, Y.; Xia, Y. *Angew. Chem. Int. Ed.* **2007,** 119, 9439-9442.
4. Wu, X.; Chen, Z.; Lu, G. Q. M.; Wang, L. *Adv. Funct. Mater.* **2011,** 21, 4167-4172.
5. Han, X.; Kuang, Q.; Jin, M.; Xie, Z.; Zheng, L. *J. Am. Chem. Soc.* **2009,** 131, 3152-3153.
6. Liu, L.; Gu, X.; Ji, Z.; Zou, W.; Tang, C.; Gao, F.; Dong, L. *J. Phys. Chem. C* **2013,** 117, 18578-18587.
7. Green, I. X.; Tang, W.; Neurock, M.; Yates, J. T. *Science* **2011,** 333, 736-739.
8. Lazzeri, M.; Vittadini, A.; Selloni, A. *Phys. Rev. B* **2001,** 63, 155409.
9. Klimeš, J.; Bowler, D. R.; Michaelides, A. *Phys. Rev. B* **2011,** 83, 195131.
10. Long, R.; Mao, K.; Ye, X.; Yan, W.; Huang, Y.; Wang, J.; Fu, Y.; Wang, X.; Wu, X.; Xie, Y.; Xiong, Y. *J. Am. Chem. Soc.* **2013,** 135, 3200-3207.
11. Yu, J.; Low, J.; Xiao, W.; Zhou, P.; Jaroniec, M. *J. Am. Chem. Soc.* **2014,** 136, 8839-8842.